

Contents lists available at ScienceDirect

# Data in Brief





## Data Article

Ultra-small cobalt particles embedded in titania by ion beam synthesis: Additional datasets including electron microscopy, neutron reflectometry, modelling outputs and particle size analysis



Abdulhakim Bake a,b, Md Rezoanur Rahman a, Peter J. Evans c, Michael Cortie d, Mitchell Nancarrow b, Radu Abrudan e, Florin Radu e, Yury Khaydukov f, Grace Causer a, Karen L. Livesey g, Sara Callori h, David R.G. Mitchell b, Zeljko Pastuovic c, Xiaolin Wang a, David Cortie a,c,\*

- <sup>a</sup> Institute for Superconducting and Electronic Materials, University of Wollongong, North Wollongong, NSW 2519, Australia
- <sup>b</sup> Electron Microscopy Centre, Innovation Campus, University of Wollongong, North Wollongong, NSW, 2519, Australia
- <sup>c</sup>The Australian Nuclear Science and Technology Organisation, Lucas Heights, NSW, 2232, Australia
- <sup>d</sup> School of Mathematical and Physical Sciences, Faculty of Science, University of Technology Sydney, Ultimo 2007, Australia
- e BESSY, Hahn-Meitner-Platz Ultra-small cobalt particles embedded 1, D-14109 Berlin, Germany
- <sup>f</sup> Max Planck Society, Outstation at the MLZ, 85748 Garching Germany/Max Planck Institute für Festkörperforschung, Stuttgart, 70569 Germany
- <sup>g</sup> The University of Newcastle, School of Mathematical and Physical Sciences, Newcastle, NSW, 2308, Australia
- <sup>h</sup> Department of Physics, California State University, San Bernardino, CA, United States

## ARTICLE INFO

Article history:
Received 14 September 2021
Revised 26 November 2021
Available online 3 December 2021

#### ABSTRACT

This Data-in-brief article includes datasets of electron microscopy, polarised neutron reflectometry and magnetometry for ultra-small cobalt particles formed in titania thin films via ion beam synthesis. Raw data for polarised neutron reflectometry, magnetometry and the particle size distribution are included and made available on a

DOI of original article: 10.1016/j.apsusc.2021.151068

\* Corresponding author.

E-mail address: dcortie@uow.edu.au (D. Cortie).

Keywords:
Cobalt nanoclusters
Ion implantation
In-situ heat treatment
Superparamagnetic
Neutron spin asymmetry

public repository. Additional elemental maps from scanning electron microscopy (SEM) with energy dispersive spectroscopy (EDS) are also presented. Data were obtained using the following types of equipment: the NREX and PLATYPUS polarised neutron reflectometers; a Quantum Design Physical Property Measurement System (14 T); a JEOL JSM-6490LV SEM, and a JEOL ARM-200F scanning transmission electron microscope (STEM). The data is provided as supporting evidence for the article in Applied Surface Science (A. Bake et al., Appl. Surf. Sci., vol. 570, p. 151068, 2021, DOI 10.1016/j.apsusc.2021.151068), where a full discussion is given. The additional supplementary reflectometry and modelling datasets are intended to assist future scientific software development of advanced fitting algorithms for magnetization gradients in thin films. Crown Copyright © 2021 Published by Elsevier Inc.

This is an open access article under the CC BY-NC-ND license (http://creativecommons.org/licenses/by-nc-nd/4.0/)

## **Specifications Table**

Subject Specific subject area Type of data Physical sciences

Surfaces and interfaces/condensed matter physics

This data includes various forms of characterization performed for nanoscale thin films of TiO<sub>2</sub> implanted with cobalt nanoparticles. A full description of the methods and experimental design is given in the Experimental section. The datasets are outlined below.

Dataset 1: 1 × Image of surface EDS mapping (Analysed)

Dataset 2:  $3 \times \text{Figs.}$  of magnetometry data (Raw)

Dataset 3: 1 × Fig. of polarised neutron spin asymmetry

Dataset 4:  $1 \times Fig.$  of polarised neutron spin asymmetry at variable temperatures

Dataset 5:  $1 \times \text{Fig.}$  of additional polarised neutron datasets for samples with different implantation conditions

Dataset 6: 1 × Fig. of numerical modelling output theoretically predicting

field-cooled and zero-field response

Dataset 1 was acquired using a Scanning Electron Microscopy equipped with an energy dispersive spectroscopy detector (JSM-6490LV, JEOL).

Dataset 2 was acquired using a 14 T Physical Property Measurement System (Quantum Design) equipped with the vibrating sample magnetometry (VSM) module.

Datasets 3 and 4 were acquired using the NREX polarised neutron reflectometer installed at the FRMII Research Reactor, Munich.

Dataset 5 contains additional polarised neutron reflectometry (PNR) measurements obtained from the PLATYPUS neutron reflectometer at the OPAL reactor, based at the Australian Nuclear Science and Technology Organisation (ANSTO).

Dataset 6 was obtained by analysing transmission electron microscopy image for a sample cross-section in high angle annular dark-field (HAADF) imaging mode on a [EOL-ARM200F microscope.

Dataset 7 was acquired using theoretical numerical calculations which took the particle histograms and magnetic anisotropy as input parameters to predict the field-cooled and zero-field cooled magnetic thermal behavior as described in Ref. [1].

(continued on next page)

How data were acquired

Data format

Parameters for data collection

Datasets 1-7) are provided as processed and datasets plotted in this document. Additional raw datasets are available in text format for Datasets 2-7) on the linked repository at <a href="https://data.mendeley.com/datasets/d2ycdfx6mz/4">https://data.mendeley.com/datasets/d2ycdfx6mz/4</a>. The reflectometry datasets from the PLATYPUS instrument are also provided in hdf5 format which contains all of the relevant additional metadata. The .hdf format is a hierarchical open access scientific format, which can be read either using the Python HDF library or by using the free hd5 viewer (available from <a href="https://www.hdfgroup.org/downloads/hdfview">https://www.hdfgroup.org/downloads/hdfview</a>).

Dataset 1 SEM-EDS mapping: SEM elemental distribution mapping was acquired while the electron beam incident angle was at 50 degrees to the specimen surface. EDS mapping was collected with the accelerating voltage set to 15 kV and the spot-size set to 60, and the SEM specimen stage was tilted to 50°. This setting helped maximise the Co dopant X-ray signal as the detected X-rays are primarily emitted from the near-surface region owing to the beam interaction volume.

Dataset 2 Magnetometry: The field-cooled (FC) magnetization was measured while warming (3-300 K) under a constant 50 Oe magnetic field after first magnetic field cooling to 3 K from room temperature under 500 Oe magnetic field. The zero-field cooled (ZFC) curve was recorded while warming (3-300 K) under a constant 50 Oe magnetic field after first cooling to 3 K from room temperature under 0 Oe magnetic field. During the magnetometry data collection, before each zero-field cooling step, the magnetic field was set to 20000 Oe, then set to 0 Oe using an oscillating approach to degauss the magnet.

Dataset 3-4 Polarised neutron reflectometry: (PNR) data were recorded at 5, 150, and 300 K using the NREX reflectomer at FRMII Munich and the PLATYPUS reflectometer at ANSTO. Additional details are given in the Methods section. The SimulReflec software was used for fitting the PNR data.

Dataset 6 Particle size histograms: A cross-sectional TEM lamella specimen was prepared by extracting a small section of the TiO<sub>2</sub> surface using standard focused-ion beam techniques. This specimen was transferred to the STEM, where it was heated in-situ up to 750 K with 50 K increment and heating rate of 10 K/min with holding time of 10 minutes. STEM images were acquired while running the in-situ heat treatment and immediately after holding at each temperature for 10 minutes. Co nanoclusters sizes were analysed with Gatan Digital Micrograph software, and at least 125 nanoclusters were measured from each image at each temperature.

Dataset 7 Numerical output of modelling: This data was calculated using the numerical model described in Ref. [1] implemented in the Mathematica software, using the experimental particle size distribution as an input parameter.

Instruments: SEM (JEOL, JSM-6490LV) coupled with Oxford Instruments' EDS detector, STEM (JEOL, ARM-200F), Gatan Digital Micrograph, Physical Properties Measurement System (Quantum Design), Platypus Neutron Reflectometer (ANSTO, Australia), NREX Neutron Reflectometer (FRMII, Germany) EDS mapping was collected while the accelerating voltage was set to 15 kV, and the SEM specimen stage was tilted to 50° to enhance the sensitivity to the surface region by reducing the beam interaction volume.

During the magnetometry data collection, before each measurement, the magnetic field was set to 20000 Oe, then set to 0 Oe using an oscillating approach to degauss the magnet. Samples were mounted on a low-background quartz rod.

For the STEM images and resulting histograms, data was collected and analysed using the high angle annular dark field detector (HAADF). This mode offers enhanced contrast primarily from variation in the atomic Z number between Co and Ti.

Polarised neutron reflectometry data was collected on two neutron instruments: NREX and PLATYPUS. NREX is a monochromatic instrument based at FRMII. PLATYPUS is a time-of-flight instrument based at the Australian Nuclear Science and Technology Organisation. A more detailed description is given in the experimental and methods section.

Description of data collection

(continued on next page)

Data source location	Institution: Institute of Superconducting and Electronic Materials, University of Wollongong
	City/Town/Region: North Wollongong/ New South Wales
	Country: Australia
Data accessibility	Repository name: Mendeley
	Data identification number: https://doi.org/10.17632/d2ycdfx6mz.4
	Direct URL to data: https://data.mendeley.com/datasets/d2ycdfx6mz/4
Related research article	A. Bake et al., "Structure and magnetism of ultra-small cobalt particles
	assembled at titania surfaces by ion beam synthesis," vol. 570, p. 151068, 2021.
	https://doi.org/10.1016/j.apsusc.2021.151068

## Value of the Data

- This data supports the claim of a method to synthesise ultra-small metallic cobalt nanomagnets embedded in titania. The value is primarily in detailing the methodology used to fabricate ultra-small Co nanomagnets that are free from oxidation, and the current methodology can be followed and fine-tuned to synthesise ultra-small size of Co nanomagnets with a higher magnetic moment. Moreover, the comprehensive characterization techniques provide a roadmap for how to detect and measure these in future work.
- Additionally, the particle size description and magnetometry measurements can be used to develop the more sophisticated theory of the unusual particle superparamagnetism. This data may provide the starting point for future theories describing the effect of a temperaturedependent saturation magnetization for ultra-small particles with a distribution of Curie temperatures.
- The neutron reflectometry datasets are described and stored in the repository which will allow other groups to repeat the analysis of the neutron reflectometry dataset. They will be useful as the input to develop more advanced analysis procedures and software. Unlike typical reflectometry of discrete homogenous thin film layers, this data describes a continuous smooth Gaussian distribution of magnetization, which makes it a valuable test case for developing advanced fitting routines for complex magnetic depth profiles. This will be a useful model scenario for developing advanced algorithms including genetic evolutionary algorithms, Monte Carlo sampling and machine learning tools for polarised neutron reflectometry problems.
- Scientific programmers developing advanced reflectometry fitting software can therefore use the dataset to validate and refine their methodology for systems with magnetization gradients
- The reflectometry data, together with the microscopy in the main text also provide a direct measurement of the stopping profile of the cobalt ion irradiation which can be used to improve Monte Carlo dose calculations for ion-beam/matter interactions.

## 1. Data Description

Dataset 1 SEM-EDS mapping: From the EDS analysis of the surfaces shown in Fig. 1, the atomic percentage of each element from the raw quantification is 77.5%, 16.4%, 5.5%, 0.6% for Si, O, Ti, and Co, respectively. The exact percentage of light oxygen cannot be accurately determined by EDS, so the actual value will differ considerably from the measured experimental value in this case, however the ratios of the transition metals are correct. The values reflect the weighted average in the beam-interaction volume, with a large component from the Si substrate owing to the micrometer electron penetration depth. The primary purpose of the EDS mapping is to show that Co ions are successfully doped and are distributed homogeneously. It is worth mentioning that the EDS mapping was performed while the sample was tilted to 50° relative to the electron

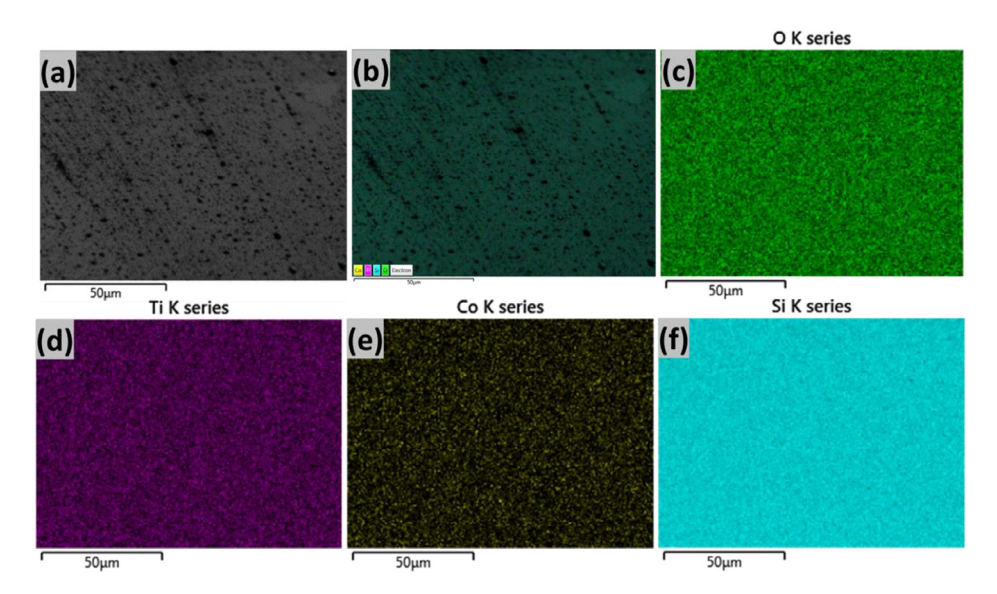


**Fig. 1.** Energy dispersive spectroscopy (EDS) mapping of the Co-doped  $TiO_2$  thin films. (a) Secondary electron image, (b) EDS layered image, and (c) - (f) are elemental maps of O, Ti, Co, and Si, respectively.

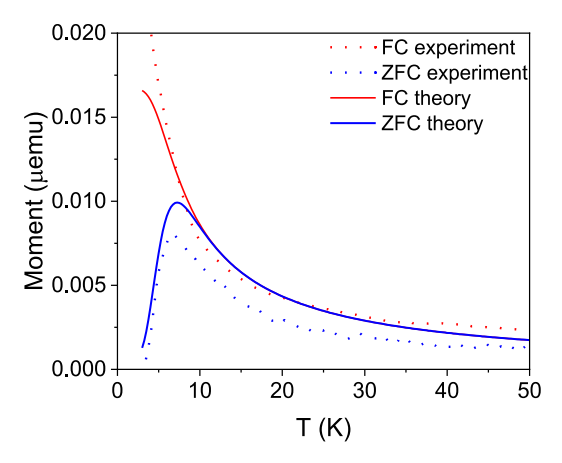


**Fig. 2.** Plot of the experimental FC/ZFC magnetometry data, overlaid with the results from the numerical model. The dotted lines are the experimental data, and solid lines are the output from the numerical model (see also Dataset 7).

beam. This is necessary to increase the Co X-ray signal as electron beam interaction volume shifts towards the surface where the majority of Co dopants are.

Dataset 2 Magnetometry: Fig. 2 shows the experimentally measured blocking temperature of the cobalt nanoclusters from the field-cooled (FC) zero-field cooled (ZFC) curves, in good agreement with the theoretically calculated blocking temperature based on the model in ref. [1], and overlaid as solid colored lines in the plot. Fig. 3 shows almost identical MvsH loops recorded for magnetic field sweeping rates from 2-100 Oe/s. This indicates there is no measurable sweep-rate dependency in the magnetization. Furthermore, the loops are all centred and symmetric around zero field, showing the absence of a detectable exchange bias. Fig. 4 shows the temperature-dependent superparamagnetic behaviour of the cobalt nanoclusters.

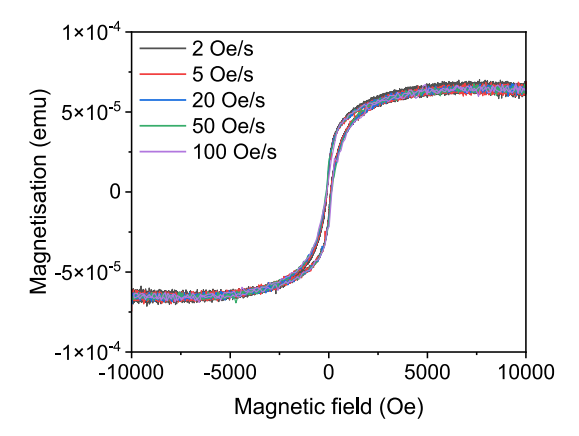


Fig. 3. Magnetisation versus magnetic field measured using different field-sweeping rates (2-100 Oe/s) at 3K.

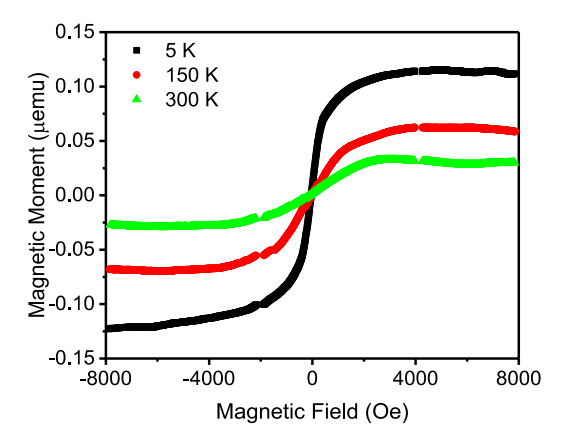
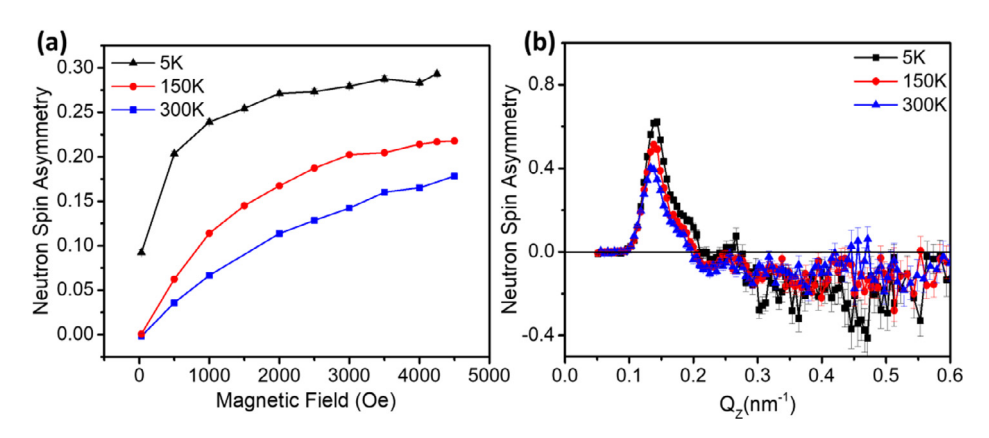
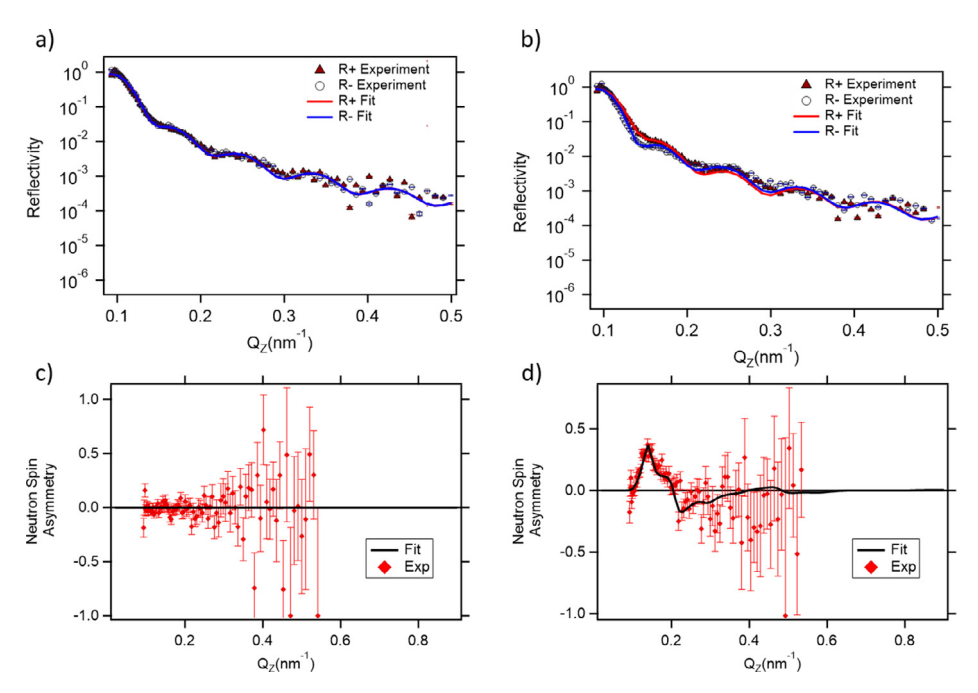


Fig. 4. Magnetisation versus magnetic field for the heat-treated sample (denotated as sample S2 in the main article).



**Fig. 5.** (a) Magnetic field dependency of the neutron spin asymmetry, (b) Temperature dependency of the neutron spin asymmetry for the multi-energy implanted sample (denotated as sample S2 in the main article).



**Fig. 6.** (a) Polarised neutron reflectometry data for a lightly doped sample with 3.5 cobalt atomic % at 10 K at 4000 Oe. (b) Polarised neutron reflectometry data for a moderately implanted sample with 5 atomic % cobalt at 10 K at 4000 Oe. The data are the points and the solid lines are the fits. (c) Spin asymmetry for the 3.5% dataset (d) Spin asymmetry and fit for the 5% dataset.

Dataset 3-4 Polarised neutron reflectometry: Fig. 5 (a) shows the neutron spin asymmetry versus magnetic field curves at the temperature of 5, 150, and 300 K measured on the NREX reflectometer for a Co-implanted TiO<sub>2</sub> film. Fig. 5 (b) shows the temperature dependency of the neutron spin asymmetry. This magnetism is linked to the cobalt ion and particle distribution. The raw data for the reflectometry curves, including those in the main article, are also contained in the linked data repository.

Dataset 5 Additional reflectometry measurements: To confirm the link between the detectable neutron spin asymmetry and cobalt distribution, Dataset 6 presents polarised neutron reflectometry for two samples with different levels of cobalt implantation. To be specific, Fig. 6 shows additional polarised neutron reflectometry measurements for samples implanted with 3.3 and 5 atomic % of Co, respectively, measured at 10 K on the PLATYPUS reflectometer in an applied field of 4000 Oe (400 mT). The samples were prepared using a single implantation step at 40 keV of cobalt, obtaining 66 KPS and 100 KPS on the dose counter, respectively. These correspond to fluences of approximately  $6.6 \times 10^{15}$  ions/cm<sup>2</sup> and  $1 \times 10^{16}$  ions/cm<sup>2</sup>. The neutron spin asymmetry (SA) profiles obtained from the data above, using the formula given in the Methods section, are shown on Fig. 6c. These illustrate the transition between a non-magnetic and magnetic state as the cobalt fluence is increased above a critical threshold. The raw data is provided in two ways in the repository: as hdf5 files and ASCII files. Firstly, the raw data files for the reflected and direct beams are provided in hdf5 format. The .hdf format is a hierarchical open access scientific format, which can be read either using the Python HDF library or by using the free hd5 viewer (available from https://www.hdfgroup.org/downloads/hdfview). It has the merits of storing all of the data and metadata (eg. sample temperatures, analyzer angles, slit sizes) which can be used to recreate the experiment. A Jupyter notebook is provided to explain how the data is processed and reduced from the hdf files. For simplicity, the key data (i.e. the reduced reflectometry curve) has also been pre-extracted from the HDF and uploaded in a separate ASCII format file.

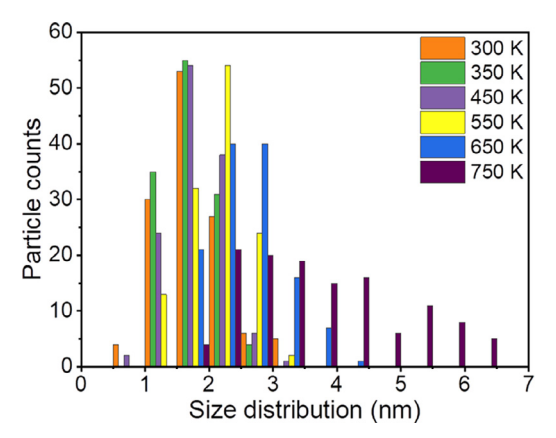


**Fig. 7.** Size distribution of the Co nanoparticles with respect to the in-situ STEM heating temperature, a minimum of individual 125 particles sizes were analysed for each temperature. Note the values are binned in increments of 0.5 nm, and the centres of the bins lie at the position between the two tick marks. Within each bin, which has boundaries as designated by the tickmarks on the x-axis, several temperatures are plotted grouped, and all of these refer to the same respective size bin. This facilitates comparison of the size distribution sampled at the same size bin but at different temperatures.

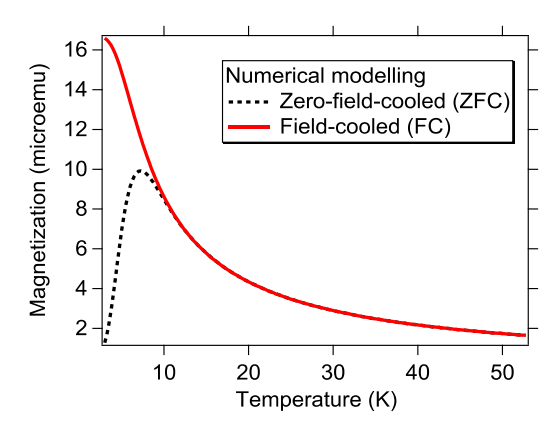


**Fig. 8.** The output of the numerical model predicting the magnetization for field-cooled and zero-field cooled cobalt ensembles, with the particle size distribution selected to match the experimental values for an as-prepared sample (300 K) in Fig. 7. This can also be compared with the experimental measurements in Fig. 2.

Dataset 6 Particle size histograms: Fig. 7 shows the cobalt nanoclusters size after heat treatment at different temperatures. The histograms show the size distribution of the cobalt nanoclusters at each temperature extracted by measuring feature sizes from the STEM images.

Dataset 7 Output of the numerical model describing the thermal magnetic response: Fig. 8 shows the theoretically calculated magnetic moment versus temperature after field cooling or zero-field cooling. This uses the particle sizes (from Fig. 7) and the anisotropy constant of  $K_A = 4.5 \times 10^6 \, {\rm erg/cm^3}$  as the input parameters. The mathematical details of the model are fully explained in Ref. [1]. Note that, while the model captures the basic trend including the ZFC cool peak, the experimental data and theoretical data do not perfectly overlap. In particular, the theory data shows a convergence of the FC and ZFC data at higher temperatures, which would be the case for standard superparamagnetic particles. In the experiment, the FC and ZFC do not converge,

and this is attributed to a saturation magnetization in the ultra-small particles which becomes temperature-dependent owing to the lower Curie point in the particles. This effect is not captured in the standard model described in Ref. [1], and the data is provided as-is, to enable improved theoretical modelling of this effect in the future which is beyond the scope of the current work.

# 2. Experimental Design, Materials and Methods

Aim and design: Previous work had established the ability to form cobalt nanomagnets using ion beam implantation (see the main article at reference [2] and references therein). This work aimed to extend these studies to provide improved insights into the structure and magnetism of the particles, whilst increasing the particle-particle spacing and decreasing the particle size. To achieve this, and also enable better STEM imaging of individual particles, the ion beam irradiation conditions were modified to distribute the cobalt more homogenously over a larger depth, and therefore create smaller, more discrete particles. In particular, multiple ion beam energies (20 and 60 keV) were used. These were selected based on Monte Carlo modelling of the penetration depth of ions and chosen to give a broader Gaussian cobalt distribution. In addition, the larger particle-particle spacing was hypothesized to modify the magnetic properties, and for this reason, a detailed study of the superparamagnetism was also performed.

## 2.1. Summary of key steps in the methodology

- Deposition of 70 nm thick amorphous TiO<sub>2</sub> thin films on Si(100-orientated) substrates using atomic layer deposition at 300 K.
- 2. Implantation of the TiO<sub>2</sub> layers using cobalt ions with incident energies of 20 and 60 keV at variable fluences to embed cobalt particles within the titania layers.
- 3. After implantation, the samples were studied using elemental mapping and surface imaging in a scanning electron microscope equipped with energy dispersive spectroscopy.
- 4. Magnetometry of the samples was performed from 300 K–5 K to detect the magnetization of the cobalt particles. The experimental data were fitted to a mathematical model.
- 5. A small piece of the sample was cross-sectioned and studied using high-resolution STEM. Histograms of the particles sizes were generated by measuring many individual particles embedded in the titania layer using cross-sectional STEM images.
- 6. The samples were studied using polarized neutron reflectometery to measure the characteristic low-angle scattering, in order to reveal the layer structure and magnetic depth profile of the cobalt particles in the titania layer.
- 7. The neutron scattering data was treated and fitted to a quantitative mathematical model.

#### 2.2. Material details

 ${
m TiO}_{2-\delta}$  films were deposited on (100)-oriented Si substrates using the atomic layer deposition (ALD) technique at 300 K. The thickness of the  ${
m TiO}_{2-\delta}$  layers was 68  $\pm$  2 nm. This thickness was selected so that the implanted layer could be well-isolated within the titania layer, away from the substrate and surface regions. Previous work on these samples has shown that the layers are amorphous for 393 K deposition and with an off-stoichiometry parameter of  $\delta \sim 0.05$  [3]. The original 2-inch diameter silicon wafer was mounted in the ALD chamber for thin film deposition. After the  ${
m TiO}_2$  layers were deposited and irradiated with cobalt, this wafer was sectioned into two 20  $\times$  20 mm pieces for PNR analysis, and a smaller piece (5  $\times$  5 mm) was cut for magnetometry.

## 2.3. Low energy ion beam synthesis of embedded particles

The  $TiO_{2-\delta}$  films were subsequently implanted with Co ions with multiple beam energies, using an ion implanter equipped with a metal vapour vacuum arc (MEVVA) ion source. The primary beam energies used were 20 keV with  $(3.3 \times 10^{15} \text{ ions/cm}^2)$  [33 kps] and 60 keV with  $1 \times 10^{16} \text{ ions/cm}^2$  [100 kps] fluences to create a more uniform ion-implanted layer within the film. Monte Carlo calculations of the ion beam stopping depths were performed using the SRIM software [4]. Two samples were synthesised with very similar conditions. The first sample (labelled S1) was fabricated without a post-implantation heat treatment to avoid recrystallisation of the films and to limit diffusion of the Co ions. Sample 2 (S2) was subjected to a gentle thermal treatment up to 450 K for 24 hours. The doses in each sample were within 10% of each other. To explore other heating regimes, rapid heating studies were also conducted on S1 using an in-situ TEM heating stage. Finally, to investigate the correlation between the magnetic properties and cobalt fluence, the results are also compared with previous implants performed at  $6.6 \times 10^{15} \text{ ions/cm}^2$  and  $1 \times 10^{16} \text{ ions/cm}^2$  at a single energy of 40 keV.

## 2.4. SEM imaging and EDS mapping

Electron images and EDS mapping was collected for the  $TiO_2$  surfaces, while the accelerating voltage was set to 15 kV, and the SEM specimen stage was tilted to  $50^{\circ}$  to enhance the sensitivity to the surface region by reducing the beam interaction volume. To analyse the SEM images and quantify the EDS maps, the Aztec software from Oxford Instruments was used.

## 2.5. Preparation of samples for cross-sectional STEM

A dual focused gallium ion beam (FIB)-SEM (FEI HELIOS NanoLab G3 CX) coupled with a gas Injection system (GIS) was used to prepare cross-sectional lamellae from the Co:  ${\rm TiO_2}$  thin films. Before FIB milling at 30 keV, approximately 1  $\mu$ m of a protective coating of carbon was deposited with an electron beam to protect the  ${\rm TiO_2}$  surface from the gallium ions. Specimens were milled to a thickness of 100 nm or less. The lamella was welded to a Cu grid ready for STEM analysis and transferred to an aberration-corrected scanning transmission electron microscope (STEM, JEOL ARM-200F) for the phase characterisation and microstructural analysis. Energy-dispersive X-ray spectroscopy (EDS) attached to the STEM was used for elemental mapping of the lamella.

#### 2.6. Scanning Transmission Electron Microscopy

The final lamella was transferred to the ARM-200F instrument for imaging. Heating was performed in-situ in a vacuum on the TEM using a heating holder. The dark field images were analysed using the DigitalMicroscope 2 (GATAN inc.) software.

# 2.7. Measurement of magnetic hysteresis and thermal response using vibrating sample magnetometry

Magnetic properties of the films were measured by a Physical Property Measurement System (PPMS) (Quantum Design, USA) using the vibrating sample magnetometry (VSM) option. The sample was mounted on a low background quartz holder with a small amount of Kapton tape positioned to give a uniform (cancelling) diamagnetic background. Before each measurement, the magnetic field was increased to 2T at room temperature and then set to zero in an oscillating approach to degauss the magnet. The data was exported to ASCII format and plotted and fitted using Origin Pro.

## 2.8. Depth-resolved magnetometry using polarised neutrons

Spin polarised neutron reflectometry is a powerful technique to measure the magnetic depth profile of the films in absolute units and reveal buried magnetic features. Initial experiments were conducted on the NREX reflectometer at the FRMII research reactor in Munich (Germany). A full description of the instrument is available at [5]. In summary, monochromatic polarised neutron beams with a wavelength of  $\lambda = 4.3$  Å were produced, and the beam was polarised using a SwissNeutronics transmission polarizer supermirror. Measurement on a calibration Fe/Si sample gave a flipping ratio approaching 1000 on the first Bragg peak showing excellent polarization. The wavelength resolution was better than 2%, and the resulting reciprocal space resolution  $\delta Qz$  was better than 0.002 Å<sup>-1</sup>. A four slit system was used to collimate the beam. The sample was aligned and mounted in a cryostat and electromagnet. The field was 4.5 kOe unless otherwise noted. Measurements were taken at 300 K and 5 K. Background subtraction was performed and the data was exported to ASCII format for fitting. Fitting was performed using the SimulReflec software package available online [8] Using this method, polarised neutron reflectometry (PNR) was used to determine the nanometer scale magnetisation per volume in the Co: TiO<sub>2</sub> thin films. The differences in the spin up (R+) and spin-down (R-) reflection patterns in PNR enabled a clear and direct observation of the magnetisation that originates from the thin implanted layer. The reflection patterns are plotted as a function of the universal scattering vector,  $Q_z = 4\pi \sin \theta/\lambda$ , where  $\theta$  is the scattering angle. The  $Q_z$  dependence of the reflection patterns provides information on the chemical and magnetic profile in the thin film. For direct qualitative analysis, it is often convenient to define a quantity, the neutron spin asymmetry (SA), which is only related to the magnetic features of the thin film, as expressed in the following form:

$$SA(Q) = \frac{R_+ - R_-}{R_+ + R_-}$$

Additional polarised neutron reflectometry was conducted on the PLATYPUS reflectometer at ANSTO. A full description of the instrument has been published previously [6]. In summary, PLATYPUS is a time-of-flight instrument, which uses neutrons in the wavelength band of 2.5 -12.5 Å (when in polarised mode). Adjustment of spinning mechanical choppers allows for variable wavelength resolution. In this work, the combination of two choppers (designated "1" and "3" on the instrument) was selected operating at 33 Hz, affording a theoretical wavelength resolution of  $d\lambda/\lambda = 3.5\%$ . A four-slit system was used to collimate the beam and provide a matching angular resolution. In fitting, the effective overall resolution of  $\delta Oz/Oz = 8\%$  was used. A Fe/Si supermirror was used to polarize the beam, which offers polarizations of 99.3%. The sample was mounted in a cryostat and aligned in a 10 kOe horizontal field provided by an electromagnet. Measurements were taken at 300 K and 10 K. Data reduction and background subtraction were performed using the FIZZY routine developed in the Igor Pro/RefNX software and exported to text format for fitting. The data was also corrected to remove the minor inefficiencies from the polarisation system, as described in the reference above. Fitting was performed using the Simul-Reflec software package, as above. During fitting, the TiO2 thickness and chemical composition of the layers were constrained to the values from the TEM imaging within a 5% uncertainty, and only the magnetization was allowed to vary.

#### **Ethics Statement**

This data was collected in accordance with the University of Wollongong framework for research integrity.

#### **CRediT Author Statement**

**Abdulhakim Bake:** Data curation, Formal analysis, Writing – original draft. **David Cortie:** Conceptualization, Data curation, Formal analysis, Writing – review & editing. **Peter Evans:** Data curation. **Michael Cortie:** Data curation, Formal analysis. **Sara Callori** and **Grace Causer:** Data curation, Formal analysis. **Radu Abrudan, Florin Radu** and **Yury Khaydukov:** Data curation, Formal analysis. **Mitchell Nancarrow:** Writing – review & editing. **Karen Livesey:** Data curation. **David Mitchell:** Data curation. **All other co-authors:** Formal analysis, Writing – review & editing.

## **Declaration of Competing Interest**

The authors declare that they have no known competing financial interests or personal relationships which have or could be perceived to have influenced the work reported in this article.

## Acknowledgments

DC acknowledges the support of the Australian Research Council (ARC) via DE180100314 and a UOW-ANSTO seed grant. This work was partly supported by the ARC Centre for Excellence in Future Low Energy Electronics (CE170100039). This research used the JEOL JEM-ARM200F funded by the ARC LIEF grant (LE120100104). Ion beam implantation was performed using the facilities at the Centre for Accelerator Science (CAS), at the Australian Nuclear Science and Technology Organisation (P7437). Research activities at the CAS including the operation of the LEII/accelerator systems are funded by the NCRIS program by the Australian Government. This work is partially based on experiments performed at the NREX instrument operated by the Max-Planck Society at the Heinz Maier-Leibnitz Zentrum (MLZ), Garching, Germany. YK would like to acknowledge the financial support of the German Research Foundation (Deutsche Forschungsgemeinschaft, DFG, Project No. 107745057 - TRR80). AB would like to thank the AINSE PGRA scholarship support.

## References

- [1] K. L. Livesey, S. Ruta, N. Anderson, D. Baldomir, R. W. Chantrell, and D. J. S. r. Serantes, Beyond the blocking model to fit nanoparticle ZFC/FC magnetisation curves, vol. 8, no. 1, pp. 1-9, 2018. doi:10.1038/s41598-018-29501-8.
- [2] A. Bake et al., Structure and magnetism of ultra-small cobalt particles assembled at titania surfaces by ion beam synthesis, vol. 570, p. 151068, 2021. doi:10.1016/j.apsusc.2021.151068.
- [3] D.L. Cortie, et al., Enhanced Magnetization of Cobalt Defect Clusters Embedded in TiO2-δ Films, ACS Appl. Mater. Interfaces 9 (10) (2017) 8783-8795, doi:10.1021/acsami.6b15071.
- [4] J.P. Biersack, L.G. Haggmark, A Monte Carlo computer program for the transport of energetic ions in amorphous targets, Nucl. Instrum. Methods 174 (1) (1980) 257–269, doi:10.1016/0029-554X(80)90440-1.
- [5] Y. Khaydukov, O. Soltwedel, T.J.J.o.l.-s.r.f.J. Keller, NREX: Neutron reflectometer with X-ray option, vol. 1, p. 38, 2015. doi:10.17815/jlsrf-1-30.
- [6] T. Saerbeck et al., Invited article: polarization "down under": the polarised time-of-flight neutron reflectometer PLATYPUS, vol. 83, no. 8, p. 081301, 2012. doi:10.1063/1.4738579.
- [8] URL: https://www-llb.cea.fr/prism/programs/simulreflec/simulreflec.html. Accessed November 25, 2021.